Scientia Horticulturae 331 (2024) 113155

Contents lists available at ScienceDirect

Scientia Horticulturae

journal homepage: www.elsevier.com/locate/scihorti

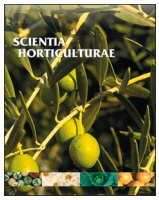

Image analysis with deep learning for early detection of downy mildew in grapevine

Inés Hernández [a,b], Salvador Gutiérrez [c,*], Javier Tardaguila [a,b]

[a] Televitis Research Group, University of La Rioja, Logroño, 26006, Spain
[b] Institute of Grapevine and Wine Sciences, (University of La Rioja, Consejo Superior de Investigaciones Cientiticas, Gobierno de La Rioja), Logroño, 26007, Spain
[c] Department of Computer Science and Artificial Intelligence (DECSAI), Andalusian Research Institute in Data Science and Computational Intelligence (DaSCI), University of Granada (UGR), Granada, 18014, Spain

ARTICLE INFO

Keywords:
viticulture
early detection
deep learning
explainable artificial intelligence

ABSTRACT

Downy mildew is a major disease of the grapevine that can severely reduce crop quality and yield. Its assessment in the laboratory is time-consuming, usually carried out by experts, and can require expensive and complex tools. For this reason, there is an opportunity to apply sensor technologies and artificial intelligence to plant disease detection. In this study, deep learning applied to RGB images was investigated to early detect downy mildew and the infection stage in grapevine leaf discs under laboratory conditions. Leaf discs of Tempranillo grapevine variety from 3 to 9 days post-inoculation located in Petri dishes were imaged using controlled conditions. Leaf disc images were extracted using computer vision techniques. Convolutional Neural Networks were used to classify the infected and healthy discs and to identify the disease infection. 10-fold cross-validation was used to evaluate the network results and Grad-CAM was used to interpret model prediction. An accuracy around 99% and a f1-score of 0.99 was achieved in downy mildew detection after DPI 3. An accuracy of 81% and a f1-score of 0.77 was obtained in infection stage identification. The developed method offered objective, rapid and accurate results, giving the possibility of early detecting downy mildew in grapevine leaf discs using low-cost techniques.

1. Introduction

Grapevine downy mildew is an important disease caused by the oomycete *Plasmopara viticola*, affecting plants and plots exponentially due to its rapid spreading with favorable conditions (Buonassisi et al., 2017). This leads to significant impact in terms of resources and environment, as it can shrink the vineyard size if not treated, or provoke an excessive use of chemicals if these are not properly directed. This disease is therefore a major concern for winegrowers, especially in the context of climate change (Bois et al., 2017; Bove et al., 2020). The traditional approaches for disease control in vineyards involve the costly supervised monitoring by experts and the frequent fungicide applications, being the latter harmful to the environment, and also prone to pathogen resistance if used massively (Massi et al., 2021). Taking advantage of sensing technologies and powerful advances in artificial intelligence, these challenges can be addressed by automated disease detection through optical sensors, including thermal readers, fluorescence sensors, and red-green-blue (RGB) imaging (Zhang et al., 2019).

Analysis of RGB images, as it involves the processing of colour distribution and pixel patterns and textures, has shown promise for detecting symptoms of downy mildew in grapevine leaves, especially when applying the latest advances in artificial intelligence and deep learning (Li et al., 2021). Deep learning is a powerful branch of artificial intelligence that has reformulated the approach to complex tasks in machine learning. It is based on artificial neural networks, that are able to automatically learn complex representations and hierarchies of features from large amounts of data. Their potential has been exploited by many authors in several fields, including plants and agriculture (Jahanbakhshi et al., 2020; Khosravi et al., 2021; Yang and Xu, 2021). Within deep learning, one of the most successful applications of neural networks for computer vision are convolutional neural networks (CNNs). These networks rely on the concept of convolution in image processing, and allow for the automated feature extraction from sample images, reducing the need for manual image pre-processing or engineering (Kamilaris and Prenafeta-Boldú, 2018b). The capability of CNNs for the extraction of relevant, high-level features from the images—without the active need of human expertise or domain kownledge—has proven useful in agriculture (Kamilaris and Prenafeta-Boldú,

* Corresponding author.
E-mail address: salvaguti@decsai.ugr.es (S. Gutiérrez).

https://doi.org/10.1016/j.scienta.2024.113155
Received 30 July 2023; Accepted 25 March 2024
Available online 29 March 2024

2018a), and particularly in plant disease detection (Abade et al., 2021).

Disease detection has been attempted with non-destructive sensors in several crops and conditions. Spectral sensing has been successfully applied for the early estimation of powdery mildew in wheat (Khan et al., 2021; Xuan et al., 2022), squash (Abdulridha et al., 2020) or (Chandel et al., 2021). Thermal technologies combined with hyperspectral imagers has been also proven useful for disease detection in cucumber leaves (Zhao et al., 2016) or rapeseed (Baranowski et al., 2015). Nevertheless, the highest reported sensing technology is arguably RGB imaging, as it can be easily deployed and symptoms can be automatically analyzed by deep learning algorithms. Examples can be found for multiple diseases in apple (Bansal et al., 2021; Jiang et al., 2019), sugar beet (Adem et al., 2023) or potato leaves (Mahum et al., 2023; Rashid et al., 2021). While reports on downy mildew detection has been already published under different conditions with RGB sensing (Bierman et al., 2019; Gutiérrez et al., 2021; Hernández et al., 2022; Zendler et al., 2021; Zhang et al., 2022), we find an opportunity for the monitoring and estimation of downy mildew in grapevine leaves as the disease grows, under the same conditions that those from Hernández et al. (2022), which assessed downy mildew severity with fuzzy logic. The current paper therefore hypothesises that RGB sensors and deep learning could be used to detect downy mildew at an early stage and to detect the infection stage in continuous monitoring. Consequently, the aim of this paper was to model RGB vine leaf images with deep learning for continuous monitoring of downy mildew from pre-inoculation to full infection after several days post-inoculation.

2. Materials and methods

2.1. Dataset generation

Part of the dataset employed was introduced by Hernández et al. (2022) under the name *Set-2*. In order to generate the dataset for training and validation, 50 grapevine plants (Vitis vinifera L., cv. Tempranillo) were grown in 5 L pots in a climate chamber at $23 \pm 2^{\circ}$ C and 80% relative air humidity. Leaf discs of 15 mm diameter were extracted from one to three leaves taken from each plant and placed on Petri dishes. Approximately half of each plant's discs (half of the Petri dishes) were inoculated with Plasmopara viticola (Toffolatti et al., 2016) and incubated in humid chamber at $23 \pm 2^{\circ}$ C for 9 days. Inoculated leaf discs were treated as positive (infected) samples, while the rest was considered as negative (healthy) samples.

During the inoculation period, RGB images (6000x4000 pixels, Fig. 1) from Petri dishes were taken, specifically on days 3 and 4 post-inoculation (DPI), when symptoms were not visible and when symptoms started to appear, respectively, and from DPI 7 to 9, when disc severity was medium to high. The images were taken using a Sony a7-II mirrorless camera (Sony Corp., Tokyo, Japan) mounting a Vario-Tessar FE 24-70 mm lens and with controlled illumination conditions. A total of 34 Petri dishes (275 leaf discs, approximately nine per dish) were imaged each day, discarding some of them due to leaf disc damages over the course of the days. Table 1 gathers the detailed information of number of samples per DPI.

2.2. Image pre-processing

Leaf disc localisation and extraction for each Petri dish was the first required step in order to work with individual disc images, similarly to Hernández et al. (2022). First, the original RGB colour space was transformed into HLS (hue, lightness, saturation) for better differentiation between the leaf discs and the Petri dish. Then, two filters were applied to smooth the HLS images while maintaining the edges and preserving the shape of the discs. The first filter applied was the initial step of mean shift segmentation with a spatial window radius of 15 pixels and a colour window radius of 30 pixels. Then, a median blur filter with a kernel of 11 pixels was applied to the saturation channel. Finally, Hough Circle Transform was used for the localisation of the centre and radius of each disc in the saturation channel (Yuen et al., 1990). The

Table 1
Number of Petri dishes and discs per day post-inoculation (DPI) and separating negative (healthy) and positive (infected) samples. The total number of discs for each type of sample is given in the last column.

Sample type	Number of samples per DPI					
	3	4	7	8	9	Total
Positive Petri dishes	18	14	14	8	8	62
Negative Petri dishes	16	16	16	11	10	69
All Petri dishes	34	30	30	19	18	131
Positive discs	147	124	108	79	71	529
Negative discs	128	128	124	115	101	596
All discs	275	252	232	194	172	1125

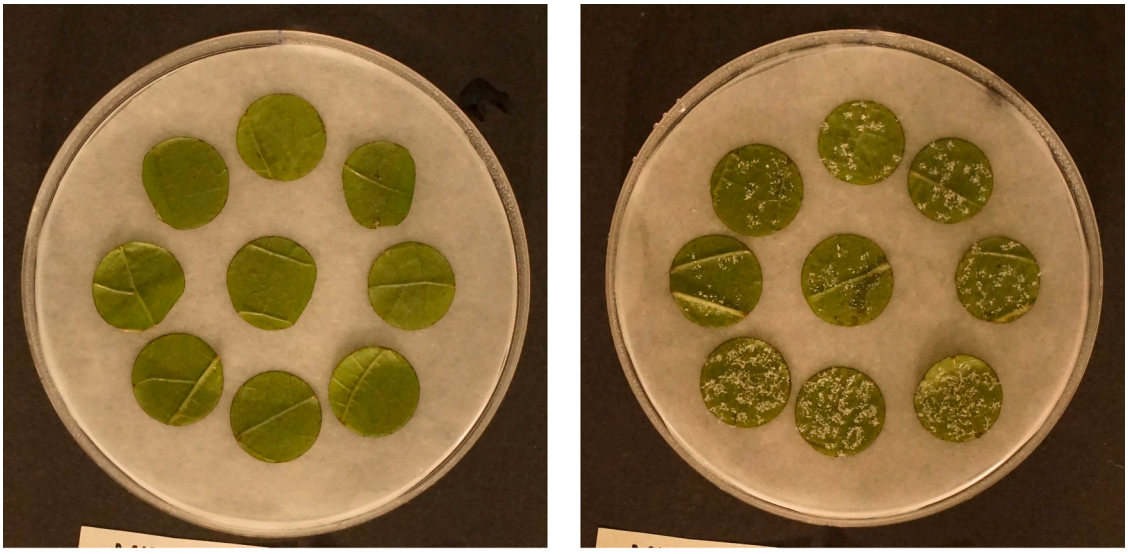

a) Negative b) Positive

Fig. 1. Examples of negative (a) and positive (b) Petri dishes from 9 days post-inoculation (DPI).

parameters for disc detection were a distance between disc centres of 150 pixels, a disc radius between 125 and 147 pixels and an upper threshold of Canny detector of 100. In addition, the leaf discs were found automatically in each image changing the inverse ratio between 1 and 4 and the threshold for centre detection between 13 to 120.

Once the discs were located, an image was extracted for each leaf disc from its radius and centre, fitting the image to the disc boundaries (Fig. 2). In view of the information provided by changing the colour space, both RGB and HLS images of the discs were taken into account. In addition, to try to reduce the complexity of the problem, masks were extracted from the discs with the detection of the most intense areas in the saturation channel both with a crisp threshold at the value 98, and with a fuzzy threshold using a trapezoidal membership function in the range of 92 to 104. To extract these masks the images were previously pre-processed, using the saturation channel from the HLS images, applying a median blur filter with a kernel of 3-pixel size and applying the Contrast Limited Adaptive Histogram Equalization method (CLAHE). As not perfect circles were delimited by Hough Circle Transform, each disc radius was reduced by 10 pixels, discarding most of the background.

2.3. Deep learning modelling

All machine learning modelling in this study was performed via transfer learning using the Convolutional Neural Network (CNN) architecture VGG16 pretrained with images from the ImageNet dataset (Simonyan and Zisserman, 2015). The input of the network was 300x300x3, considering the maximum detail of the disc images. The models were trained minimizing the cross-entropy loss in a maximum of 1000 epochs using a batch size of 64 and the Adam optimizer, reducing the learning rate from 10^{-5} to 10^{-9} by a factor of 0.1 if the validation loss stopped improving after 50 epochs. The models were evaluated using the accuracy, f1-score, precision and recall metrics. False positive and false negative values were also evaluated to analyse the error of the models. RGB images, HLS images, crisp masks and fuzzy masks were used independently for their comparison to check which gave the most information for detecting and identification of downy mildew infection. Moreover, the training data was augmented using an online data augmentation to reduce overfitting, applying random transformations on the images such as vertical and horizontal flipping, rotation in a range between 0 and 360 degrees and a 50% increase and decrease in brightness. Both training and validation images were normalized to the range from zero to one, to make the training of the model faster.

2.3.1. Early downy mildew detection

In order to check whether it was possible to detect downy mildew infection in an early stage, the data from the fourth day post-inoculation was selected, when the first visual symptoms started to appear as sporulation in the abaxial side of the leaf discs. This data was used to make a 10-fold cross-validation to evaluate the general network performance and check if it was possible to differentiate the positive and the negative discs automatically. An early stopping mechanism was used to stop the training when the model stop improving after 200 epochs, using the model with the less validation loss as the final model.

Once all the models used in the cross-validation were trained, all the data from the 4 DPI was used to train a model, considering the average number of epochs used to obtain the best model in each fold as the maximum epoch. This model was used to evaluate the generalization of the method, validating them with the data from all the DPIs independently, analysing the disease detection on each day and each type of image pre-processing. To provide interpretability to the model prediction and see which parts of the leaf discs were more or less important to the neural network in detecting the disease, Gradient-weighted Class Activation Mapping (Selvaraju et al., 2019) was employed.

2.3.2. DPI identification

On the other hand, to detect whether it was possible to differentiate the stage of infection of the disease, an attempt was made to identify to which DPI a leaf disc corresponded once the infection was detected by its visual symptoms. For this approach, positive discs (infected by downy mildew) from DPI 4 to 9 were used to make a 10-fold cross-validation, in a similar way as for early detection. In this case, only the types of image pre-processing that gave the best results in detecting the infection of the discs were compared. Confusion matrix was used to evaluate the correct and wrong predictions in each DPI and possible confusions between days.

3. Results

3.1. Early downy mildew detection

During the incubation period, symptoms were first visible very slightly in DPI 4. For this day, four different kinds of modeling were developed using different images as input: full RGB; full HLS; crisp mask;

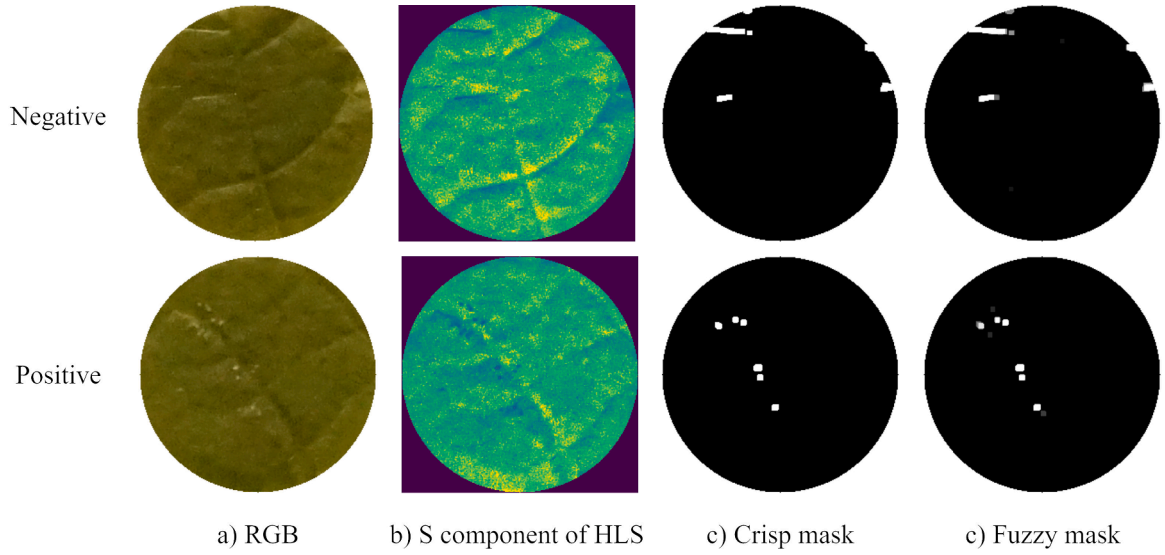

Fig. 2. Examples of images of negative (healthy) and positive (infected) discs processed. RGB image (a), HLS image (b), crisp mask (c) and fuzzy mask (d) were considered.

and fuzzy mask. The results from the 10-fold cross-validation of this DPI are summarized in Table 2. Average accuracy and precision validation values were all at around 90%, reaching 98% by those models trained with HLS images. The F1 score, although classes were almost completely balanced in DPI 4, showed that no bias existed towards any of the two classes. On the other hand, looking at the number of epochs needed to train the network, it can be seen that by using masks, starting from less information about the discs, the models needed fewer epochs to train, although using RGB or HLS images this information helped to obtain a better classification.

To analyse the behaviour of the neural networks during the training process, charts of the accuracy evolution per epoch are displayed in Fig. 3. Evolution plots of the CNN trainings show quick convergence between training and validation lines in all four cases. In the case of the RGB and HLS images (Fig. 2a and b), both training and validation lines reached their maximum convergence before 50 epochs, and after it lines run almost in parallel, with a slight divergence along the epoch increase. In contrast, the modelling that involve masks presented a divergence with an increased growth rate (Fig. 2c and d). Still, they reached their peak performance (the epoch in which both training and validation lines begin to diverge) virtually at the same point than the plots in the first row of Fig. 2.

Given the good prediction capability obtained from the models trained with data from DPI 4, complete CNN models were trained using all samples from that day and the previously listed types of input images. With these four models, leaf disc images from the remaining DPIs were predicted and their performance statistics computed and presented in Table 3. The original number of imaged leaf discs began diminishing since inoculation, due to sample deterioration (like damage or necrosis), especially in the last DPIs (as disease evolved). This caused an increased class imbalance in DPIs 8 and 9. Excluding DPI 3 and 4, classification results from the remaining DPIs (7, 8 and 9, with abundant visible symptoms) reached or surpassed accuracy values of 97%. The prediction of the images from DPI 4 resulted in lower classification accuracies than latter DPIs, but still above 93%. Models from crisp and fuzzy masks in DPI 4 yielded the higher number of false negatives (17 and 15, respectively, both out of 124 positive samples). Finally, for DPI 3 the models gave completely inaccurate results, as precision values around the 0.50 mark and high false negative values reflected the prediction of almost all discs as negative discs.

The neural network trained with the RGB images was analysed and processed using Grad-CAM. Results per DPI are presented in Fig. 4 for a single leaf disc image during disease evolution. In the case of the latter DPIs (7, 8 and 9, with higher levels of visual symptoms), the CNN focused primarily on the top half of the disc, that matches with the fact that downy mildew spots accumulated on the same zones. Still, spot clusters on the bottom semicircle also received an increased importance as disease advanced. Regarding DPI 4, although symptoms were clearly less distinguishable than the next imaged DPI, the neural network was able to detect and give special importance to those zones with downy mildew spots (Fig. 4, second column), whether scattered-top half or concentrated-bottom right.

Table 2
Results from the 10-fold cross validation of the leaf disc modelling at DPI 4. The last column represents the average number of epochs, per fold, needed by the neural network to converge into the highest accuracy.

Input type	10-fold cross validation				
	Accuracy (%)	Precision	Recall	F1-score	Epochs
RGB	97	0.97	0.97	0.97	280
HLS	98	0.98	0.98	0.98	293
Crisp mask	88	0.88	0.88	0.88	78
Fuzzy mask	90	0.90	0.90	0.90	151

3.2. DPI identification

The RGB and HLS images were chosen to detect the stage of infection of the discs by the DPI to which they belonged, as this type of data seemed to provide more information to the network in the early detection. Multi-class modelling for the classification between the different DPIs was developed and validated using a 10-fold cross validation for RGB and HLS images. The confusion matrices and statistics are gathered in Table 4. The best accuracy was obtained using the RGB leaf disc images (81% vs 77%). Precision, recall and F1 scores were fairly similar, within rows in Table 4 and also between image input (RGB and HLS). This was caused by the different misclassification rates that occurred between the three latter DPIs. Additionally, it is worth noting that samples of DPI 4 were almost perfectly classified, and very few of them were misclassified (and when it occurred, the predicted label was DPI 7). A high precision is also maintained for DPI 7, even though some of the discs are mainly classified as the latest DPIs. On the other hand, DPIs 8 and 9 are mainly confused with each other and with DPI 7, because sporulation at these stages was very similar.

4. Discussion

Early detection when the symptoms started to appear was achieved with high accuracy for each type of input. The use of masks that highlighted areas with higher saturation values helped to focus the detection on the symptoms and required less time for the model to converge. In addition, the fuzzy mask gave slightly better results by providing more information about the intensity of the highlighted areas, also discussed in Hernández et al. (2022). However, the masks reflected some false positives due to nerves in the leaves or water droplets reflecting similar saturation in the image, unlike the work of Gutiérrez et al. (2021), where thresholding seemed to favour the detection of downy mildew and spider mite. Thus, the RGB and HLS images seemed to provide more information about the infection, giving better results and less overfitting during neural network training, suggesting that models trained with these data are suitable for accurately detecting downy mildew symptoms in the early stages of infection, when sporulation became visible. This reflected the good performance of using CNNs for downy mildew detection with very low severity without applying pre-processing to the images or adjusting disease thresholds for the masks, as in Chandel et al. (2021) or Hernández et al. (2022), taking advantage of the use of transfer learning and data augmentation to obtain good results with a reduced amount of data. These techniques have already proven to work better than machine learning-based approaches on datasets collected in the laboratory such as detecting plant diseases using the PlantVillage dataset (Kumar et al., 2022), achieving an accuracy of 99.64%, or detecting defects in sour lemons (Jahanbakhshi et al., 2020), achieving an accuracy of 100%. This was also demonstrated in this case for the detection of downy mildew in early stages under laboratory conditions, although the symptoms were barely visible.

When the model trained with the most troubled discs, where symptoms were hardly visible, was used on other days, the DPIs that have symptoms (4, 7, 8 and 9) were correctly detected, even though the level of infection was not considered during training. This reflected the robustness of the method, which differed from other works such as Khan et al. (2021), where powdery mildew was detected in wheat at pre-symptomatic stages, but the imbalance in the number of diseased and healthy leaves caused errors in the classification of late stages of the disease. The results were almost similar to those that could be obtained using a visible and near infrared spectral system (Baranowski et al., 2015; Zhang et al., 2019) to detect plant disease symptoms, which would be more costly and complex to process than using RGB imaging. On the other side, when the symptoms were not visible, such as in the DPI 3, the model was not capable of detecting the infection. Therefore, these techniques could be combined with other systems using fluorescence or thermal sensors to detect pre-symptomatic stages of the disease,

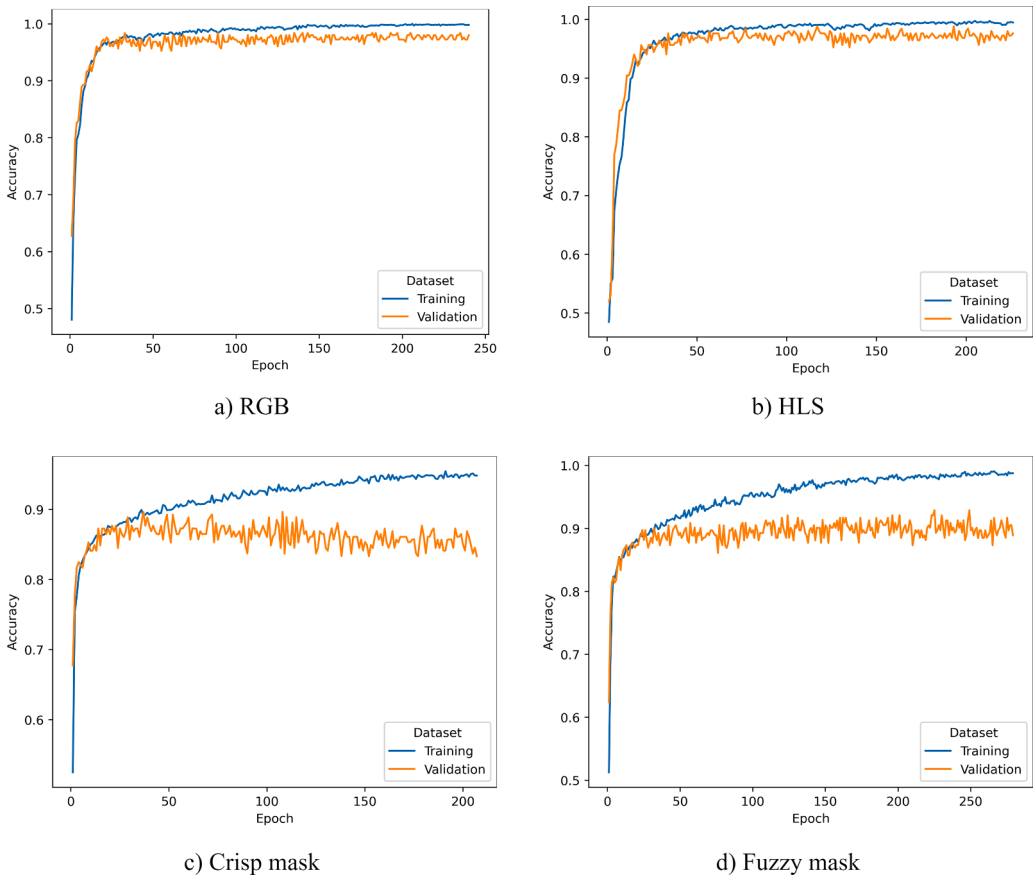

Fig. 3. Evolution of the CNN in the modelling of DPI 4 (10-fold cross-validation) with four different image inputs: RGB (a); HLS (b); crisp mask (c); and fuzzy mask (d). The ordinate represents the average accuracy in the epoch from all folds.

Table 3
Classification results in the prediction of leaf disc images from days post-inoculation (DPI) 3, 4, 7, 8 and 9, using four different kinds of inputs (RGB; HLS; crisp mask [BM]; and fuzzy mask [FM]). The prediction model was trained with images from DPI 4 (first visible symptoms).

DPI	Input type	Accuracy (%)	Precision	Recall	F1-score	FP	FN	Number of discs	
								Positive	Negative
3	RGB	47	0.51	0.50	0.35	5	141	147	128
	HLS	48	0.56	0.51	0.38	6	136		
	CM	53	0.61	0.55	0.47	10	120		
	FM	48	0.57	0.51	0.37	4	139		
4	RGB	100	1.00	1.00	1.00	0	0	124	128
	HLS	100	1.00	1.00	1.00	0	0		
	CM	93	0.94	0.93	0.93	1	17		
	FM	94	0.95	0.94	0.94	0	15		
7	RGB	100	1.00	1.00	1.00	0	1	108	124
	HLS	99	0.99	0.99	0.99	0	2		
	CM	97	0.97	0.97	0.97	1	6		
	FM	98	0.98	0.98	0.98	0	5		
8	RGB	100	1.00	1.00	1.00	0	0	79	115
	HLS	99	0.99	0.99	0.99	1	1		
	CM	99	1.00	0.99	0.99	0	1		
	FM	99	0.99	0.99	0.99	0	2		
9	RGB	99	1.00	0.99	0.99	0	1	71	101
	HLS	99	0.99	0.99	0.99	1	1		
	CM	98	0.99	0.98	0.98	0	3		
	FM	99	0.99	0.99	0.99	0	2		

such as the infection in DPI 3. In addition, the detection with RGB images could be interpreted by the results obtained with the Grad-CAM method, as a novelty to other works where CNNs were also employed, such as its use to detect diseases in apple leaves (Bansal et al., 2021) or to estimate the severity of powdery mildew in grapevine (Bierman et al., 2019). With this method, it was observed that the model ignored the infection on symptomless discs, but on the other stages it focused on practically all the sporulation, giving importance to the areas of the discs showing symptoms of downy mildew to perform the classification. Thus, it can be concluded that the symptoms could be detected in the discs when they were visible using RGB images, or data extracted from this type of images using deep learning models, even in the first days, but for

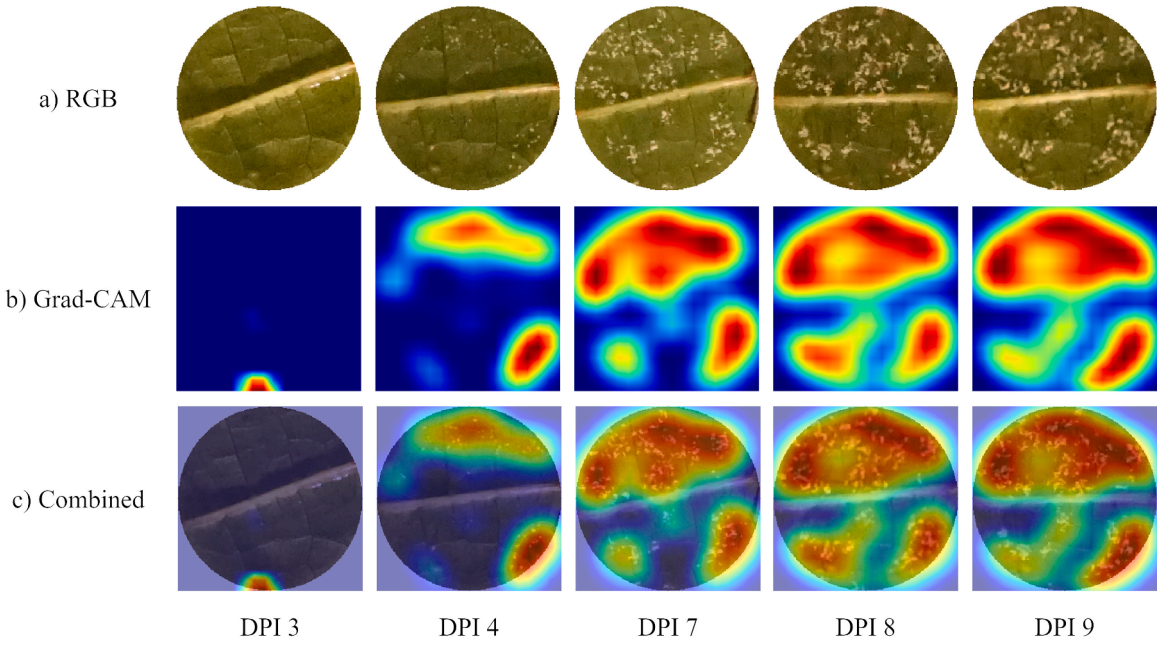

Fig. 4. Results from Grad-CAM using the model trained with RGB leaf diss images from the DPI 4. The example shows the RGB image of a disc at DPIs 3 to 9 (a), the heatmap resulting from the Grad-CAM method (b) and the combination of both (c). The reddish zones represent the features that the model considers more relevant for classification.

Table 4
Results for the 10-fold cross validation of DPI classification using RGB and HLS disc images. Correctly classified samples and its precision in percentage (diagonal of the confusion matrix) are highlighted. Epochs refers to the average number of epochs the models needed for training during the 10-fold cross validation.

Input type			Confusion matrix				Accuracy (%)	Precision	Recall	F1-score	Epochs
			Predicted DPI								
			4	7	8	9					
RGB	Actual DPI	4	**123 (99%)**	1	0	0	81	0.77	0.77	0.77	150
		7	2	**96 (85%)**	11	4					
		8	0	8	**49 (62%)**	22					
		9	0	11	15	**45 (63%)**					
HLS		4	**123 (99%)**	1	0	0	77	0.74	0.73	0.73	135
		7	2	**93 (82%)**	10	8					
		8	0	15	**47 (59%)**	17					
		9	0	18	17	**36 (51%)**					

detecting the asymptomatic stages it could be necessary its combination with other sensors.

When trying to differentiate the stage of the infection, it was possible to differentiate with high accuracy the day with early symptoms of the disease (DPI 4), but the rest of the days became confusing to classify, especially the last days which had very similar symptoms and were confused between them. This indicates that this method was very good at distinguishing the early from the late stages of infection (after day 7 post inoculation), and in many cases could also differentiate DPI 7 (with more than 80% accuracy), where the symptoms are slightly less than in DPIs 8 and 9, which are almost completely confused with each other or with DPI 7. Furthermore, in this case the RGB images performed better than the HLS, especially in the classification of the last days of infection, which seems to indicate that by not processing these images less information about the discs was lost which helped to differentiate the stages of infection. Another way to obtain disease stage could be to estimate the severity by detecting sporulation on leaf discs, as in the case of Zendler et al. (2021), where a shallow convolutional neural network was used, or in the case of Hernández et al. (2022), where computer vision and fuzzy logic were used. However, in both cases, an expert assessment of each disc indicating the level of infection was necessary, unlike in this work, where the classification was done by its DPI, which reduced the data labelling time. In addition, the estimation of severity often reflects various false positives due to leaf nerves, water droplets or leaf hairs, which seemed to be reduced by classifying the discs. In Abdulridha et al. (2020) the stage of powdery mildew disease in squash was considered using hyperspectral images taken in the laboratory, which allowed more information to be extracted from data such as chlorophyll concentration, plant water content or leaf cell structure. However, in addition to the economic cost of these sensors and the amount of time and specialized personnel needed to handle and analyse the data, the detection of the disease when it presented early symptoms made certain errors and the stages of the disease needed to be monitored separately due to the difference in their features. The method developed in this work provided accurate disease detection even when symptoms were early and disease stage differentiation between early (DPI 4), intermediate (DPI 7) and high (DPI 8 and 9) using RGB images, which could be obtained with low-cost sensors, and are easy to analyse using deep convolutional neural networks, requiring little data pre-processing.

5. Conclusion

Applying deep learning to RGB images enabled automatic detection of early symptoms of downy mildew in grapevine leaves in the

laboratory, allowing to evaluate different treatments in an easy and rapid way. The developed method demonstrated its capability of detecting disease symptoms since the fourth day after inoculation, considering the sporulation on the leaves. Using convolutional neural networks facilitate data preprocessing, achieving high accuracy using raw data, which implied less time in giving a diagnostic of the leaf discs. Moreover, transfer learning helped facilitating automatic feature extraction of disc images, using previous knowledge of the model. On the other hand, automatic DPI identification was performed differentiating when the symptoms started to appear, from the 7 DPI and the last days. This differentiation could facilitate the identification of the first symptoms and the late stages of the infection, adding information about the infection detected to evaluate possible treatments applied. This work showed the usefulness of deep learning techniques for early detection of plant diseases in the laboratory and the identification of their stage of infection with data that could be acquired easily and cheaply, even with a mobile phone.

Declaration of competing interest

The authors declare that they have no known competing financial interests or personal relationships that could have appeared to influence the work reported in this paper.

Acknowledgments

This work has been developed as part of the project NoPest (Novel Pesticides for a Sustainable Agriculture), which received funding from the European Union Horizon 2020 FET Open program under Grant agreement ID 828940. Inés Hernández would like to acknowledge the research funding FPI grant 1150/2020 by Universidad de La Rioja and Gobierno de La Rioja.

References

Abade, A., Ferreira, P.A., de Barros Vidal, F., 2021. Plant diseases recognition on images using convolutional neural networks: a systematic review. Comput. Electron. Agric. 185, 106125.

Abdulridha, J., Ampatzidis, Y., Roberts, P., Kakarla, S.C., 2020. Detecting powdery mildew disease in squash at different stages using uav-based hyperspectral imaging and artificial intelligence. Biosyst. Eng. 197, 135–148.

Adem, K., Ozguven, M.M., Altas, Z., 2023. A sugar beet leaf disease classification method based on image processing and deep learning. Multimedia Tool. Appl. 82, 12577–12594.

Bansal, P., Kumar, R., Kumar, S., 2021. Disease detection in apple leaves using deep convolutional neural network. Agriculture 11, 617.

Baranowski, P., Jedryczka, M., Mazurek, W., Babula-Skowronska, D., Siedliska, A., Kaczmarek, J., 2015. Hyperspectral and thermal imaging of oilseed rape (brassica napus) response to fungal species of the genus alternaria. PloS One 10, e0122913.

Bierman, A., LaPlumm, T., Cadle-Davidson, L., Gadoury, D., Martinez, D., Sapkota, S., Rea, M., 2019. A high-throughput phenotyping system using machine vision to quantify severity of grapevine powdery mildew. Plant Phenomic. 2019.

Bois, B., Zito, S., Calonnec, A., 2017. Climate vs grapevine pests and diseases worldwide: the first results of a global survey. OENO One 51, 133–139.

Bove, F., Savary, S., Willocquet, L., Rossi, V., 2020. Simulation of potential epidemics of downy mildew of grapevine in different scenarios of disease conduciveness. Eur. J. Plant Pathol. 158, 599–614.

Buonassisi, D., Colombo, M., Migliaro, D., Dolzani, C., Peressotti, E., Mizzotti, C., Velasco, R., Masiero, S., Perazzolli, M., Vezzulli, S., 2017. Breeding for grapevine downy mildew resistance: a review of "omics" approaches. Euphytica 213, 1–21.

Chandel, A.K., Khot, L.R., Sallato, B., 2021. Apple powdery mildew infestation detection and mapping using high-resolution visible and multispectral aerial imaging technique. Scientia Horticulturae 287, 110228.

Gutiérrez, S., Hernández, I., Ceballos, S., Barrio, I., Díez-Navajas, A.M., Tardaguila, J., 2021. Deep learning for the differentiation of downy mildew and spider mite in grapevine under field conditions. Comput. Electron. Agric. 182, 105991.

Hernández, I., Gutiérrez, S., Ceballos, S., Palacios, F., Toffolatti, S. L., Maddalena, G., Diago, M. P., Tardaguila, J., 2022. Assessment of downy mildew in grapevine using computer vision and fuzzy logic. Development and validation of a new method.

Jahanbakhshi, A., Momeny, M., Mahmoudi, M., Zhang, Y.D., 2020. Classification of sour lemons based on apparent defects using stochastic pooling mechanism in deep convolutional neural networks. Scientia Horticulturae 263, 109133.

Jiang, P., Chen, Y., Liu, B., He, D., Liang, C., 2019. Real-time detection of apple leaf diseases using deep learning approach based on improved convolutional neural networks. IEEE Access 7, 59069–59080.

Kamilaris, A., Prenafeta-Boldú, F.X., 2018. Deep learning in agriculture: a survey. Comput. Electron. Agric. 147, 70–90.

Kamilaris, A., Prenafeta-Boldú, F.X., 2018. A review of the use of convolutional neural networks in agriculture. J. Agric. Sci. 156, 312–322.

Khan, I.H., Liu, H., Li, W., Cao, A., Wang, X., Liu, H., Cheng, T., Tian, Y., Zhu, Y., Cao, W., et al., 2021. Early detection of powdery mildew disease and accurate quantification of its severity using hyperspectral images in wheat. Remote Sens. 13, 3612.

Khosravi, H., Saedi, S.I., Rezaei, M., 2021. Real-time recognition of on-branch olive ripening stages by a deep convolutional neural network. Scientia Hortic. 287, 110252.

Kumar, R., Chug, A., Singh, A.P., Singh, D., 2022. A systematic analysis of machine learning and deep learning based approaches for plant leaf disease classification: a review. J. Sensor. 2022.

Li, L., Zhang, S., Wang, B., 2021. Plant disease detection and classification by deep learning-a review. IEEE Access 9, 56683–56698.

Mahum, R., Munir, H., Mughal, Z.U.N., Awais, M., Sher Khan, F., Saqlain, M., Mahamad, S., Tlili, I., 2023. A novel framework for potato leaf disease detection using an efficient deep learning model. Hum. Ecol. Risk Assess.: Int. J. 29, 303–326.

Massi, F., Torriani, S.F., Borghi, L., Toffolatti, S.L., 2021. Fungicide resistance evolution and detection in plant pathogens: plasmopara viticola as a case study. Microorganisms 9, 119.

Rashid, J., Khan, I., Ali, G., Almotiri, S.H., AlGhamdi, M.A., Masood, K., 2021. Multi-level deep learning model for potato leaf disease recognition. Electronics 10, 2064.

Selvaraju, R.R., Cogswell, M., Das, A., Vedantam, R., Parikh, D., Batra, D., 2019. Grad-CAM: visual explanations from deep networks via gradient-based localization. Int. J. Comput. Vis. 128, 336–359.

Simonyan, K., Zisserman, A., 2015. Very deep convolutional networks for large-scale image recognition. hrefhttp://arxiv.org/abs/1409.1556arXiv:1409.1556.

Toffolatti, S.L., Maddalena, G., Salomoni, D., Maghradze, D., Bianco, P.A., Failla, O., et al., 2016. Evidence of resistance to the downy mildew agent plasmopara viticola in the georgian vitis vinifera germplasm. Vitis 55, 121–128.

Xuan, G., Li, Q., Shao, Y., Shi, Y., 2022. Early diagnosis and pathogenesis monitoring of wheat powdery mildew caused by blumeria graminis using hyperspectral imaging. Comput. Electron. Agric. 197, 106921.

Yang, B., Xu, Y., 2021. Applications of deep-learning approaches in horticultural research: a review. Hortic. Res. 8.

Yuen, H., Princen, J., Illingworth, J., Kittler, J., 1990. Comparative study of hough transform methods for circle finding. Image Vis. Comput. 8, 71–77.

Zendler, D., Malagol, N., Schwandner, A., Töpfer, R., Hausmann, L., Zyprian, E., 2021. High-throughput phenotyping of leaf discs infected with grapevine downy mildew using shallow convolutional neural networks. Agronomy 11, 1768.

Zhang, J., Huang, Y., Pu, R., Gonzalez-Moreno, P., Yuan, L., Wu, K., Huang, W., 2019. Monitoring plant diseases and pests through remote sensing technology: a review. Comput. Electron. Agric. 165, 104943.

Zhang, Z., Qiao, Y., Guo, Y., He, D., 2022. Deep learning based automatic grape downy mildew detection. Front. Plant Sci. 13, 872107.

Zhao, Y.R., Li, X., Yu, K.Q., Cheng, F., He, Y., 2016. Hyperspectral imaging for determining pigment contents in cucumber leaves in response to angular leaf spot disease. Sci. Rep. 6, 27790.